

Conformational Transitions of Spherical Polymer Brushes: Synthesis, Characterization, and Theory

Douglas Dukes,[†] Yu Li,^{‡,||} Sarah Lewis,[†] Brian Benicewicz,^{‡,||} Linda Schadler,[†] and Sanat K. Kumar^{*,§}

[†]Department of Materials Science & Engineering, and [‡]Department of Chemistry, Rensselaer Polytechnic Institute, 110 8th Street, Troy, New York, and [§]Department of Chemical Engineering, Columbia University, New York, New York. ^{||}Current address: Department of Chemistry and Biochemistry, University of South Carolina, Columbia, SC.

Received June 8, 2009; Revised Manuscript Received November 30, 2009

ABSTRACT: We examine the structure of densely grafted polymer layers grown from the surfaces of spherical nanoparticles over a broad range of graft densities and chain lengths. Dynamic light scattering (DLS) experiments show that the hydrodynamic thickness of the polymer layer, h , scales as $h \propto N^{4/5}$ for short chains and high grafting densities, that is, in the concentrated polymer brush (CPB) regime, whereas $h \propto N^{3/5}$ for long enough chains (semidilute polymer brush, SDPB). The mean field theory of Wijmans and Zhulina is able to collapse approximately all of our data and those in the existing literature (even on other polymers) into an apparently universal form. From these findings, we conclude that the result $h \propto N^{4/5}$ for the CPB is an intermediate crossover scaling, relevant to particles of finite curvature, analogous to the $h \propto N$ observed for concentrated flat brushes. Second, the scaling $h \propto N^{3/5}$ uniquely reflects the increased space available to the chain segments as one proceeds away from a curved grafting surface. Under these situations, the chains experience less packing frustration as compared to a planar brush, and the semidilute polymer brush shows scaling behavior analogous to chains in good solvent, even though the chains are much more extended.

Introduction

It is now commonly accepted that the dispersion state of nanoparticles in a polymer matrix critically controls the properties of the resulting nanocomposite.¹ An intriguing method of modifying dispersion is to use nanoparticles with chains grafted to their surfaces; these chains can have the same or a compatible chemistry with the matrix.^{2,3} However, to take full advantage of this concept, it is necessary to understand how the matrix and grafted chains interact. To this end, the structure of the grafted polymer chains, alternatively known as polymer brushes, must be understood as a function of graft density and molecular weight. There has been considerable interest in this topic from both an experimental and a theoretical viewpoint.

The thickness of grafted polymer layers can show different scaling behavior in different regimes controlled by the grafting density, chain length and particle curvature. It is thus helpful to establish a clear and consistent description of these different regimes (see Table 1 summarized from the literature). At low enough molecular weight or at low enough graft density, the radius of gyration of the chains, R_g , does not exceed the inter-chain spacing. Individual chains do not interact with adjacent chains, and thus they assume mushroom-like conformations on the grafting surface (Figure 1A). Consequently, the measured brush height in this regime is $h \approx 2R_g$.⁴ Only when these “mushrooms” begin to overlap do the chains begin to behave as brushes.

In the case of planar brushes, the pioneering theoretical work of Alexander⁵ and de Gennes⁶ predicted a linear dependence of brush height, h , on the degree of polymerization, N (l_0 is the monomer length and $\sigma^* = \sigma l_0^2$ is the reduced grafting density)

$$h \propto l_0 N \sigma^{*1/3} \quad (1)$$

*Corresponding author. E-mail: sk2794@columbia.edu.

This result is valid for low-to-intermediate graft densities where the intermonomer interactions are typically pairwise (semidilute polymer brush, SDPB). At even higher graft densities, when higher order interactions become important (concentrated polymer brush, CPB), the scaling of brush height becomes^{7,8}

$$h \propto l_0 N \sigma^{*1/2} \quad (2)$$

Note that this form is derived in the limit $\sigma^* \rightarrow 1$, where the segment density profile approaches a step function. Most brushes are in the regime defined by eq 1 because it is difficult to synthesize long chains at high enough graft densities where eq 2 applies.

Spherical brushes show similar behavior in that a transition from mushrooms to SDPB to CPB is observed. There are two important differences between flat brushes and curved brushes that are worth emphasizing. First, as noted in Table 1, the N scaling of the brush height assumes a different form than for a planar brush in the SDPB regime (Figure 1B). Second, in a spherical geometry, if the chains are long enough, then brushes initially in the CPB regime will transition to the SDPB regime at some distance, r_c , from the center of the nanoparticle (Figure 1C). Note that this transition arises because the packing constraints near the surface are relaxed by the increased volume available to chains as the radial distance away from a spherical surface increases. Brushes grafted to flat surfaces cannot alleviate steric constraints in this manner and hence do not show such rich behavior with variations in chain length and grafting density. Below, we discuss the current theoretical and experimental understanding of such curved brushes.

Theory

In addition to our well-developed understanding of planar brushes, a generalized treatment for curved brushes was

Table 1. Various Behavioral Regimes of Grafted Polymers and Their Characteristics

curvature	behavior	scaling with N, σ^*	chain interactions
flat/spherical	mushroom	$N^{3/5}$	free chain in good solvent
flat	SDPB	$N^1 \sigma^{*1/3}$	pairwise, excluded volume effects
flat	CPB	$N^1 \sigma^{*1/2}$	higher-order, non-gaussian chains
spherical	SDPB	$(N \sigma^{*1/3})^{3/5}$	pairwise, excluded volume effects
spherical	CPB	$(N \sigma^{*1/2})^x, 3/5 < x \leq 1$	higher-order, non-gaussian chains

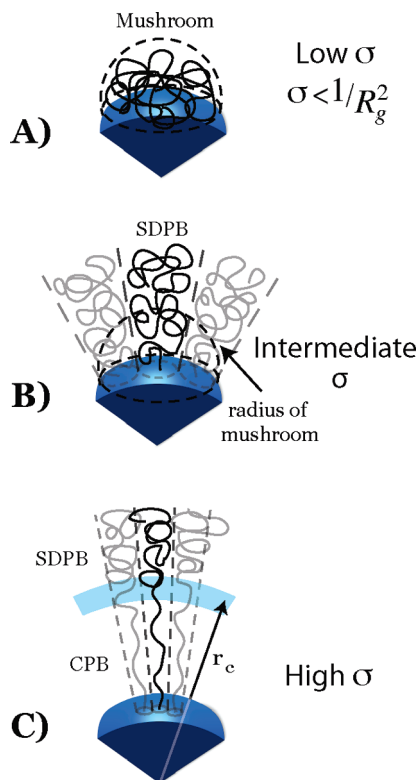


Figure 1. Schematic representation of the varied conformational behaviors of polymer brushes attached to spherical interfaces. See the text for description.

presented by Daoud and Cotton (DC), who extended the phenomenological scaling arguments of Alexander and de Gennes to the somewhat related context of star polymers.⁹ This model assumes that all chains are bonded to a central point and that the free ends extend an identical distance away. The average brush height for a spherical interface in the limit of long chains is¹⁰

$$h \propto l_0 N^{3/5} f^{1/5} v^{1/5} \equiv l_0 (N f^{1/3} v^{1/3})^{3/5} \quad (3)$$

where f is the number of arms in the star and v is the second virial coefficient, also known as the excluded volume parameter ($\equiv 1/2 - \chi$, where χ is the Flory parameter).

Ohno et al.¹¹ extended this model to treat chains grafted to a nanoparticle of radius, r_0 . They postulate the existence of a critical radius r_c , which is derived from the “star-polymer” treatment of Daoud and Cotton

$$r_c = r_0 \sigma^{*1/2} v^{*-1} \quad (4)$$

Here $\sigma^* = f l_0^2 / 4\pi r_0^2 \equiv \sigma l_0^2$ is the reduced graft density and $v^* = v / (4\pi)^{1/2}$, where v is the excluded volume parameter. This result was obtained by setting the DC expression for the chain swelling parameter, $\alpha = 1$. Therefore, for all $h + r_0 \leq r_c$, the chains are in the CPB regime, where $\alpha = 1$ (no solvent swelling). For larger h , where $\alpha > 1$ (solvent swelling), the chains crossover into the SDPB regime, yielding $h \propto N^{3/5}$ as $N \rightarrow \infty$.

We also comment here on the σ^* scaling of h . All models that only account for interactions at the pair level will yield $\sigma^{*1/3}$ scaling. The inclusion of higher-order interactions should yield $\sigma^{*1/2}$ scaling by analogy to flat brushes.^{7,8} Two points are emphasized here. First, as with the DC model, the Ohno extension assumes that the ungrafted chain ends are a uniform distance away from the grafting surface and the segment density profile is a step function. These are important assumptions that are disputed by several newer theories. Second, this theory predicts a crossover from CPB behavior to the SDPB ($h \propto N^{3/5}$) with increasing length. Again, this crossover is predicted by using only the expressions for the chain swelling parameter, α , in the semidilute limit. We will demonstrate below that the DC model works well in this limit, and hence this crossover result is robust, even though we believe that the DC model is itself inaccurate for $h + r_0 \leq r_c$. Locating this transition from CPB behavior to the SDPB limit (where $h \propto N^{3/5}$) is one aim of our work.

More recently, self-consistent field models have been used to quantify polymer brush behavior and interactions between them.^{12,13} Dan and Tirrell numerically solved the Dolan–Edwards self-consistent field equations in the vicinity of a spherical grafting surface. They found that the scaling of brush height with N varied from eqs 3 to 1 as the particle radius was systematically increased.¹³ More importantly, these workers found that the ungrafted chain ends were uniformly distributed in the brush, except for an exclusion zone near the particle surface. This picture of the distribution of chain ends is currently the accepted one in the community.

Another model that encapsulates this transition from linear to $3/5$ scaling behavior is that of Milner–Witten–Cates,¹⁴ as adapted by Wijmans and Zhulina (MWC-WZ).¹⁵ In the limit of small curvature (large particles), the brush height, h , normalized by the planar brush height, H_0 (alternatively, the effective brush height for a flat interface at an identical graft density and molecular weight), assumes the form

$$\left(\frac{h}{H_0}\right)^3 \left[1 + \frac{3}{4} \left(\frac{h}{\omega H_0}\right) + \frac{1}{5} \left(\frac{h}{\omega H_0}\right)^2\right] = 1 \quad (5)$$

where

$$H_0 = \left(\frac{8}{\pi^2}\right)^{1/3} l_0 N v^{1/3} \sigma^{*1/3}$$

$\omega = r_0 / H_0$, and v is the excluded volume parameter (second virial coefficient). As discussed above, the form of H_0 (which is derived using a pairwise approximation for planar brushes) yields $\sigma^{*1/3}$ scaling. Therefore, the σ^* scaling in the CPB will be incorrectly predicted by this model. Given this incorrect prediction, it is not clear if this model is relevant to the CPB regime of interest to us; this is a question we shall explicitly address in our work.

We now focus on the big bracketed terms on the left-hand side of the equation. Because $h / \omega H_0 \equiv h / r_0$, the limit where h / r_0 is small yields brush heights that scale linearly with that of a flat brush. As the chains increase in length (or the particle radius gets smaller), higher-order terms become more important, causing a continuous transition from the N^1 to the $N^{3/5}$ behavior. From the

form of the equation, changing the curvature will merely alter the onset of this transition; higher curvatures transition at shorter chain lengths.

Experimental Section

To investigate experimentally the scaling of the brush height with chain length and grafting density requires the ability to graft chains of a given, controlled length at any grafting density to a spherical surface. This has become a topic of considerable interest with at least two well-developed methods: the “grafting to” approach (i.e., attaching polymers to the surface) or the “grafting from” approach (initiating polymerization from the surface). The former is limited in the grafting density that can be achieved, because the grafted chains sterically inhibit further chains from attaching to the surface.¹⁶ In contrast, “grafting from” methods have the advantage of the polymerization proceeding outward from the surface of the particle, thus facilitating the growth of long-chain-length brushes, even at high grafting densities. For this reason, surface-initiated living radical polymerization techniques, such as atom transfer radical polymerization (ATRP)^{11,16–21} and reversible addition–fragmentation chain transfer (RAFT) polymerization,^{16,22–25} have proven to be useful in this context.

For spherical grafting surfaces, the pioneering experimental investigation of Savin et al.¹⁷ explored the brush height of polystyrene grown by the ATRP method from 20 nm diameter silica nanoparticles. The brush molecular weights were up to ~35 kg/mol with high surface grafting densities (~0.6 chains/nm²). Polydispersities were typically in excess of 1.2 to 1.3. Because the brush height measured by DLS appeared to vary linearly with N , these authors deduced that these brushes were in the planar scaling regime. We consider this conclusion in light of the MWC-WZ model (eq 5): the smallest brushes considered by Savin et al. were $h \approx 5$ nm, whereas $r_0 = 10$ nm. Therefore, the ratio $h/r_0 \approx 0.5$. In this regime, we might have expected intermediate scaling between $h \propto N$ and $h \propto N^{3/5}$, and hence the conclusion that the brushes are in the $h \propto N$ scaling regime is surprising. Whereas the N scaling is thus not expected to be that of a planar brush, these assemblies may still be in the CPB regime. Examination of these data on a log–log plot, as will be discussed below, will allow us to resolve unequivocally this issue. Furthermore, no evidence of $h \propto N^{3/5}$ behavior was found for these low molecular weights by these authors; they conjecture that this transition to SDPB behavior occurs at even higher molecular weights.

Experimental measurements on polymer brushes made by ATRP have frequently exceeded graft densities of 0.5 chains/nm², while the polydispersities were often > 1.3. Recently, more refined ATRP techniques have been used to synthesize PMMA brushes with polydispersities near 1.2 for molecular weights in excess of 200 kg/mol.¹¹ These brushes were grown on 130 nm diameter silica particles where the grafting densities ranged from 0.60 to 0.80 chains/nm² with molecular weights ranging from ~90 to 500 kg/mol. Using these methods, Ohno et al. demonstrated that the brushes were grafted at a sufficient density to exhibit CPB behavior at the lower molecular weights. They also predicted a transition from CPB to SDPB behavior for molecular weights beyond ~120 kg/mol.

This article builds on these previous works and uses the flexibility of the RAFT polymerization technique to synthesize spherical brushes of varying lengths with graft densities ranging from 0.05 to 0.55 chains/nm² (Table 2), grafted to 14 nm diameter silica particles.^{24,25} Using this technique, polymer brushes have been synthesized with polydispersities of < 1.15 with molecular weights in the range of 4–120 kg/mol. This broad range of brush parameters enables the examination of the scaling of the brush height with chain length and grafting density. In particular, the focus is on the transitional scaling behavior of the polymer brush from that expected for a CPB to that expected for SDPB. The $h \propto N$ scaling expected from flat brushes is not recovered for

Table 2. Graft Density and Molecular Weight of Specimens Prepared by Surface-Initiated RAFT Polymerization for This Study, Along with the Corresponding Average Brush Height As Measured by DLS

graft density σ (chains/nm ²)	molecular weight M_w (kg/mol)	PDI (M_w/M_n)	brush height h (nm)	st. dev. (nm)
0.05	34	1.05	27.98	2.90
0.05	52	1.06	41.82	3.25
0.05	95	1.10	59.75	9.55
0.39	4	1.06	6.37	0.82
0.39	6.6	1.08	9.61	6.59
0.39	13	1.06	18.02	2.24
0.39	45	1.05	49.33	2.35
0.39	74	1.10	67.31	3.40
0.39	114	1.13	91.40	2.81
0.55	26	1.06	37.61	2.38
0.55	59	1.08	66.42	2.98
0.55	77	1.09	75.89	6.41
0.55	117	1.12	100.26	6.36

brushes expected to be in the CPB regime. Rather, the brush height is found to scale as $h \propto N^{4/5}$ and eventually reaches the expected 3/5 scaling as the chain length increases (SDPB behavior). We conjecture that the $N^{4/5}$ scaling is the CPB for the nanoparticle sizes, chain lengths, and graft densities employed. The observed 4/5 scaling behavior should crossover to the $h \propto N$ behavior as σ^* gets larger at small values of h/r_0 (short brushes and large core radii). These results show the rich behavior exhibited by these spherical brushes, results that have significant practical consequences on their ability to tune the dispersion and hence the properties of polymer nanocomposites.²⁶

Methods

Synthesis. The surface-initiated RAFT polymerization process has been previously documented^{24,25} and is briefly discussed here. Silica nanoparticles (14 ± 4 nm diameter, Nissan Chemical, 30 wt % in methylethylketone) were dispersed in tetrahydrofuran (THF) (HPLC grade, Acros Organics), grafted with a silane coupling agent, and reacted with the chain transfer agent. UV–vis absorption spectra were acquired for graft density determination, and the particles were then dried and weighed. Particles were redispersed in THF and then surface-polymerized with styrene monomer (ACS grade, Acros Organics) that was passed through a neutral alumina column to remove the inhibitor. After polymerization, a sample of grafted chains was cleaved from the surface using hydrofluoric acid; the polymer molecular weight was determined by GPC using polystyrene standards.

Characterization. The grafted particle solution was redissolved in benzene (ACS grade, Acros Organics) and diluted to a concentration of ~0.05 mg/mL. DLS measurements (Dynapro Titan, Wyatt Technologies, Santa Barbara, CA) were performed on 10 different aliquots of the diluted solutions to obtain the average hydrodynamic radius. The determination of particle size by DLS is well documented in the literature and consequently will not be discussed here.²²

Results and Discussion

Experimental Results. The brush height is defined as $h = R_h - r_0$, where R_h is the hydrodynamic radius of the polymer grafted particle, and r_0 is the core radius. The brush height is shown in Figure 2 as a function of degree of polymerization, N , for the samples in Table 1. While the data in this Figure appear to suggest that the height of the long chain brushes follow the expected SDPB scaling ($h \propto N^{3/5}$), it is unclear if

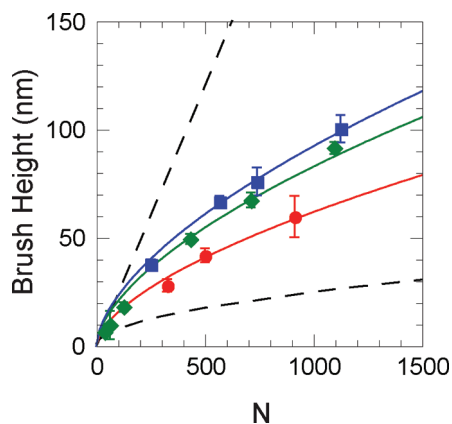


Figure 2. Brush height versus degree of polymerization with the curve fits of eq 3 indicated. Dashed lines represent fully stretched (upper bound) and ideal coil ($R_g \approx 1_0 N^{1/2}$, lower bound) chains. Red circles, green diamonds, and blue squares data for graft densities 0.05, 0.39, and 0.55 chains/nm², respectively.

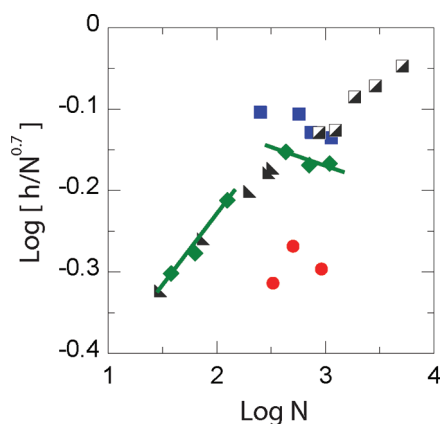


Figure 3. Plot of $h/N^{0.7}$ versus degree of polymerization, N . The legend is the same as that in Figure 2 with literature data included. The half-filled squares are the data of Ohno et al.,¹¹ whereas the inverted triangles are the data of Savin et al.¹⁷

this behavior is demonstrated by all brushes. To clarify this point, we replot the data in Figure 2 in the form $h/N^{0.7}$ versus N on a log–log basis in Figure 3.

We begin by discussing our data at a grafting density of 0.39 chains/nm². The data appear to show two distinct trends, which, by linear extrapolation, appear to cross at $N \approx 315$ (a molecular weight of roughly 33 kg/mol). We propose that this crossover represents the CPB–SDPB transition, which is apparently unique to curved brushes. We will show in Table 3 that this extrapolated crossover chain length is in excellent agreement with the crossover radius calculated from eq 4 with a ν^* value derived by fitting the MWC–WZ model to all of the brush heights. To justify this claim further, we note that for molecular weights beyond this “transition”, the data are consistent within experimental error with the expected 0.6 power law scaling. (We find $h \propto N^{0.65}$ in this regime.) The data below the transition for this grafting density appear to follow $h \propto N^{0.8}$, which is quite different from the $h \approx N$ expected for flat brushes. We speculate that these lower molecular weight data are in a crossover regime, with the planar scaling ($h \propto N$) found for $h/r_0 \rightarrow 0$, when $\sigma^* \rightarrow 1$. The linear scaling is therefore a rare condition for spherical surfaces, even rarer than the CPB itself, found only for very short chains on highly grafted surfaces with small curvature. This conjecture is consistent with the predictions of the MWC–WZ model because our lowest

Table 3. Theoretical Crossover Height for the Experimental Systems

σ	ν^*	r_c (nm)	h_c (nm)
0.05	0.2	6	–1
0.39	0.09	41	33
0.55	0.09	48	41
0.59 ¹⁷	0.04	150	140
0.7 ¹¹	0.01	4310	4245

$h/r_0 \approx 0.85$ at this graft density, a regime where we might have expected intermediate scaling between $h \propto N$ and $h \propto N^{3/5}$. Indeed, an asymptotic expansion of eq 5 to order $1/r_0^2$ suggests that the brush height assumes the form

$$h = H_0 \left(1 - \frac{H_0}{4r_0} - \frac{29}{240} \left[\frac{H_0}{r_0} \right]^2 \right)$$

in the limit $1/r_0 \rightarrow 0$. Because $H_0 \propto N$, the scaling away from $h \propto N$ is embodied by this form. A last piece of bolstering evidence is from the work of Ohno et al.¹¹ These workers have argued that their brushes are in the CPB regime and that a plot of $h[1 + (h/2r_0)]$ versus $N\sigma^{1/2}$ yields a straight line; plotting this data in the form h versus N on log–log axes yields the familiar 4/5 power law scaling, which is consistent with our results in the regime we conjecture to be the CPB. We thus believe that the $h \propto N^{0.8}$ scaling represents the CPB regime for particles of a finite curvature, and thus the intersection point in the vicinity of $N \approx 315$ corresponds to the CPB–SDPB transition.

We now note that our data for the higher grafting density, 0.55 chains/nm², also yield $h \propto N^{0.6}$. Following eq 4 for the graft density of 0.55 chains/nm² suggests that the CPB–SDPB crossover occurs for $h \approx 41$ nm. Other than the shortest h data point, all other data in these experiments are beyond this transition and are consistent with SDPB behavior in all respects. Similarly, the previous data of Savin et al.¹⁷ at a graft density of 0.59 chains/nm² are all in the $h \propto N^{0.8}$ regime because the predicted crossover ($h_c \approx 140$ nm) is much larger than the thickest brush considered by these workers. Therefore, these brushes are in the CPB regime, even though they do not obey $h \propto N$. We also note that the Ohno et al.¹¹ data follow $h \propto N^{0.8}$. However, it is difficult to estimate the crossover height because their system was PMMA grafted to much larger silica colloids, whereas all of the remaining data were for polystyrene chains on similar core radii (7.5 and 10 nm).

Our data at the lowest graft density (0.05 chains/nm²) are not consistent with the two higher graft densities. Two facets of our data are emphasized. First, assuming ν^* is constant with graft density, eq 4 predicts $h_c = 7$ nm. (Below, we show that this assumption is not valid, because a fit of the MWC–WZ model to all the brush heights at this graft density yields $\nu^* = 0.2$. Using this best fit value yields an ever smaller $h_c = -1$ nm.) Because the experimental brush heights are beyond either h_c , SDPB behavior must be found for all data at this graft density. However, only the two highest N data points appear to be consistent with a 0.6 power law scaling; the lowest-molecular-weight brush seems to follow a stronger trend than $N^{0.7}$. While this implies that this data point could be in a crossover regime into the CPB regime, this conclusion is inconsistent with our estimates for the crossover height. Possibly, the lowest h value is in error. Second, and more importantly, we observed that the apparent brush height increases the longer the samples are held in the DLS instrument. Separately, we had deduced that the nanoparticles began to aggregate noticeably in solution about 0.5 h after the aliquot preparation (which involved sonication). While

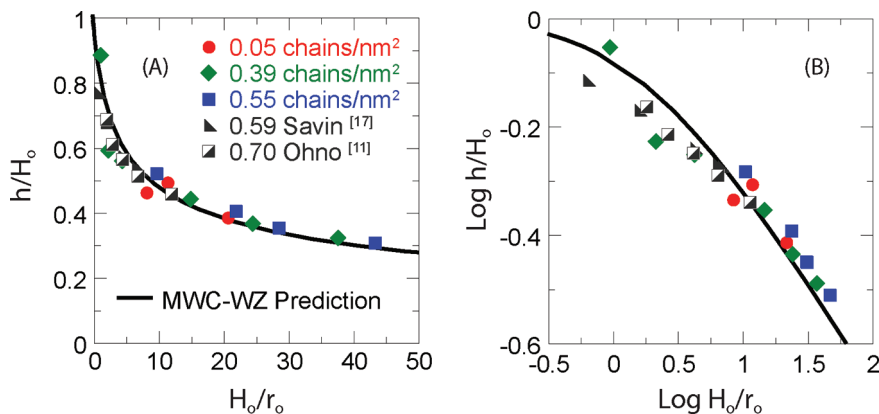


Figure 4. Normalized brush height versus normalized particle radius plotted with (A) linear and (B) logarithmic axes. H_0 is the height of a corresponding brush on a flat surface. The line is the prediction of the MWC-WZ model from eq 5.

we take great care to use only data on freshly prepared solutions where this problem is minimized, these data are not as “clean” as the other data sets under discussion here.

Comparison to Theoretical Models. We now quantitatively compare our data to the predictions of two standard models, the DC approach and the Milner–Witten–Cates theory applied to this situation by Wijmans–Zhulina (MWC–WZ). We first compare our experimental results with the MWC–WZ model. Figure 4A clearly shows that this model apparently provides an excellent description of all data from our work, that of Savin et al., and that of Ohno et al. (which is for a different polymer) on a single “master” curve. Two points are worth emphasizing here. First, the form that describes the data (namely, eq 5) was derived in the limit of large particle radii. This conclusion can be rationalized a posteriori by computing the ratio r_0/l_0 , which is on the order of 10 in our case and of Savin, whereas it is ~ 100 for the Ohno et al. experiments. Clearly, these particles are much larger than the Kuhn length of the chains, and thus potentially justify the applicability of eq 5 in this context. A second, and probably more crucial point, is that we have used the same excluded volume (second virial coefficient) parameter, $v^* = 0.09$, to describe our data at the two higher graft densities, while the lowest graft density, which we believe to be anomalous because of particle agglomeration, is fit by a very different value, $v^* = 0.2$. Additionally, we used $v^* = 0.04$ (0.59 chains/nm², where the solvent is different from our case¹⁷) and 0.01 (0.59 to 0.74 chains/nm², Ohno et al.¹¹). Using the fitted values of v^* , we calculate the theoretical crossover radius from eq 4. Therefore, the crossover brush height can be found by $h_c = r_c - r_0$, shown in Table 3. Note that the predicted crossover height, $h_c = 33$ nm, for a grafting density of 0.39 chains/nm² is in agreement with the value $h_c = 28$ nm deduced from Figure 3, suggesting the robustness of our conclusions for the CPB–SDPB transition.

Here we restate the fact that the MWC–WZ model accounts for only pairwise interactions. Therefore, it should not describe the CPB. Surprisingly, this model appears to reasonably describe the experimental data in this regime. To better understand this issue, we replot the data in a log–log form in Figure 4B. It is now clear that the MWC–WZ model works best for $H_0/r_0 > 10$, the SDPB regime, whereas for smaller values (the CPB), it systematically overpredicts the experiments. Therefore, the MWC–WZ model does a better job of predicting brush heights in the SDPB than in the CPB regime. However, this model still seems to do an adequate job of representing the CPB regime.

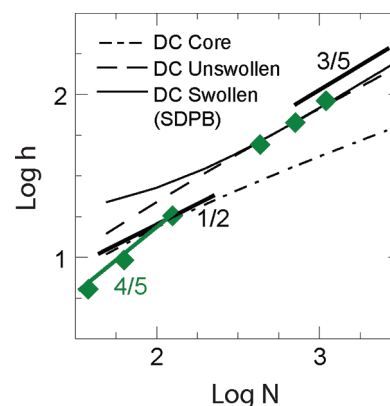


Figure 5. Brush height as a function of degree of polymerization. The points are data from a grafting density of 0.39 chains/nm². Several lines are shown (see the Appendix): the short dashed line is the DC prediction in the core region. The dashed line at intermediate N is the “unswollen” region, whereas the larger N predictions (the solid line) correspond to the $N^{3/5}$ scaling regime. The solid lines with scalings of 3/5 and 1/2 and 4/5, as indicated, are shown for reference.

Next, we consider the applicability of the DC model in the context of our experiments. We use only the data corresponding to $\sigma = 0.39$ chains/nm², our most extensive data set. From Figure 5, it is apparent that the higher chain length data, corresponding to the “swollen” or SDPB regime ($\alpha > 1$), are well described by this approach. This is not surprising given that eq 3 is derived in the high N limit. However, for shorter chain lengths, this model fails completely. As the “swollen” and “unswollen” regimes begin to deviate below r_c , the “unswollen” form fails to capture any of the experimental behavior. From the adapted forms of the DC model equations, as shown in the Appendix, the “core” (fully extended chains) and “unswollen” ($\alpha = 1$) behaviors do not yield a proper scaling at intermediate values of N . Rather than the experimentally observed scaling of $h \propto N^{0.8}$, the theory gives a much different slope, closer to 0.5. This is in disagreement with the experiments, and hence we conclude that the DC model is not appropriate for use in this context. Rather, our results unequivocally suggest that the segment density profile inherent in the MWC–WZ model is closer to the physical reality of experimental systems than the step function profile of DC.

Finally, we examine the applicability of the data analysis procedure of Ohno et al.¹¹ These researchers found that a log–log plot of $h[1 + (h/2r_0)]$ versus $\sigma^{1/2}L_c$ (where $L_c = Nl_0$ is the contour length) yielded straight lines for brushes conjectured to be in the CPB regime (Figure 6). Data from

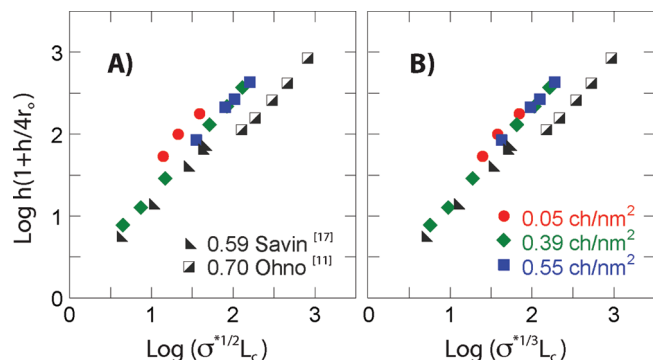


Figure 6. Comparison of the expected (A) CPB and (B) SDPB σ^* scalings using the MWC-WZ model in a form inspired by Ohno et al.¹¹

brushes on particles of very different radii (10 vs 65 nm), were found to fall on the same line describing CPB behavior.¹¹ Furthermore, this line was distinct from that for highly stretched brushes on flat surfaces.

We cannot derive the form used by Ohno from the MWC-WZ model. Instead, an examination of eq 5 shows that to leading order, $h[1 + (h/4r_0)] = H_0$. This immediately suggests that a plot of the left-hand side against $\sigma^{*1/3}L_c$ should approximately collapse all of the data for a single system (given nanoparticle with a certain grafted polymer and a fixed solvent) onto a single master curve. Because this σ^* scaling is only valid for the SDPB regime, for brushes in the CPB regime we expect that the x axis should be $\sigma^{*1/2}L_c$. Figure 6 considers all available data in these two different forms. It appears that either form collapses only parts of our data. Therefore, this plot does not resolve the σ^* dependence, and hence we cannot use this metric to ensure that our brushes in fact demonstrate the CPB-SDPB transition. Instead, we point to several other consistency checks discussed above that unequivocally demonstrate that this transition occurs, especially for the grafting density of 0.39 chains/nm², our most extensive data set.

Concluding Remarks

Over a range of polymer chain lengths, grafting densities, and core particle sizes, the experimental results demonstrate that the height of a spherically grafted polymer brush transitions from an intermediate $h \propto N^{4/5}$ dependence in the CPB regime to a $h \propto N^{3/5}$ expected in the SDPB regime. The crossover radius determined by the DC model is a self-consistent means of determining the CPB-SDPB transition. The MWC-WZ predictions of brush behavior match well with all existing experimental brush heights, especially in the SDPB regime. We speculate that the brushes in the CPB regime do not show the $h \propto N$ dependence predicted for planar brushes for two reasons. First, because of the small particles to which these chains are grafted, the ratio $h/r_0 \approx 0.5$, even for the shortest brushes considered. The treatment of MWC-WZ immediately suggests that these cases will not produce $h \propto N$ but rather a smaller power law, which is consistent with our observations. Second, if we were experimentally capable of pushing toward the limit $\sigma^* \rightarrow 1$ and investigating shorter brushes and/or larger particles, we might be able to access the flat brush-like linear scaling regime of the CPB more easily within the experimental range of the DLS technique. While this is a topic that we leave as an open challenge in this field, we reiterate the conclusion that the CPB regime on spherical particles does not require the $h \propto N$ scaling found for planar brushes.

Acknowledgment. This work was supported by the Nano-scale Science and Engineering Initiative of the National Science

Foundation under NSF award number DMR-0642573 and by NSF-0804647 (S.K.K.). This material is based on work supported under a National Science Foundation Graduate Research Fellowship.

Appendix

To compare the DC model for star polymers to a grafted nanoparticle system, the segment density profile equation (equation 17 of ref 9) was reintegrated to reflect the same profile grafted to a spherical surface at r_0 . The following equations are obtained for the three behavioral regimes: core, unswollen, and swollen.

core:

$$h = [3cNf_0^3 + r_0^3]^{1/3} - r_0$$

unswollen:

$$h = l_0 \sqrt{2cNf^{1/2} + \frac{f}{3} + \left(\frac{r_0}{l_0}\right)^3 \left(\frac{2}{3f^{1/2}}\right)} - r_0$$

swollen:

$$h = l_0 f^{1/2} v^{1/5} \left[\frac{5}{3} \left(\frac{1}{6} + \frac{cN}{f^{1/2}} + \frac{1}{10v^2} + \frac{1}{3} \left(\frac{r_0}{l_0 f^{1/2}} \right)^3 \right) \right]^{3/5} - r_0$$

These equations are plotted in Figure 5, where c is a fitting constant. These new results do not yield the experimentally observed N scaling behavior except in the SDPB regime. This might explain the lack of good agreement between this model and experiments shown in Figure 5.

References and Notes

- (1) Vaia, R. A.; Maguire, J. F. *Chem. Mater.*, **2007**, *19*, 2736–2751 and references therein.
- (2) Lin, Y.; Boker, A.; He, J.; Sill, K.; Xiang, H.; Abetz, C.; Li, X.; Wang, J.; Emrick, T.; Long, S.; Wang, Q.; Balazs, A.; Russell, T. *Nature* **2005**, *434*, 55–59.
- (3) Takai, C.; Fugii, M.; Takahashi, M. *Colloids Surf., A* **2007**, *292*, 79–82.
- (4) Wu, T.; Efimenko, K.; Vlcek, P.; Subr, V.; Genzer, J. *Macromolecules* **2003**, *36*, 2448–2453.
- (5) Alexander, S. J. *Phys. (Paris)* **1977**, *38*, 983–987.
- (6) de Gennes, P. *Macromolecules* **1980**, *13*, 1069–1075.
- (7) Shim, D. F. K.; Cates, M. E. *J. Phys. (Paris)* **1989**, *50*, 3535–3551.
- (8) Lai, P. Y.; Halperin, A. *Macromolecules* **1991**, *24*, 4981–4982.
- (9) Daoud, M.; Cotton, J. J. *Phys. (Paris)* **1982**, *43*, 531–538.
- (10) Birshtein, T. M.; Borisov, O. V.; Zhulina, Y. B.; Khokhlov, A. R.; Yurasova, T. A. *Vysokomol. Soedin., Ser. A* **1987**, *29*, 1169–1174.
- (11) Ohno, K.; Morinaga, T.; Takeno, S.; Tsujii, Y.; Fukuda, T. *Macromolecules* **2007**, *40*, 9143–9150.
- (12) Kim, J. U.; Matsen, M. W. *Macromolecules* **2008**, *41*, 4435–4443.
- (13) Dan, N.; Tirrell, M. *Macromolecules* **1992**, *25*, 2890–2895.
- (14) Milner, S. T.; Witten, T. A.; Cates, M. E. *Europhys. Lett.* **1988**, *5*, 413–418.
- (15) Wijmans, C. M.; Zhulina, E. B. *Macromolecules* **1993**, *26*, 7214–7224.
- (16) Tsujii, Y.; Ohno, K.; Yamamoto, S.; Goto, A.; Fukuda, T. *Adv. Polym. Sci.*, **2006**, *197*, 1–45 and references therein.
- (17) Savin, D.; Pyun, J.; Patterson, G.; Kowalewski, T.; Matyjaszewski, K. *J. Polym. Sci., Part B: Polym. Phys.* **2002**, *40*, 2667–2676.
- (18) Huang, X.; Wirth, M. J. *Anal. Chem.* **1997**, *69*, 4577–4580.
- (19) Husseman, M.; Malmström, E.; McNamara, M.; Mate, M.; Mecerreyes, D.; Benoit, D.; Hedrick, J.; Mansky, P.; Huang, E.; Russel, T.; Hawker, C. *Macromolecules* **1999**, *32*, 1424–1431.
- (20) Perruchot, C.; Khan, M. A.; Kamitsi, A.; Armes, S. P.; von Werne, T.; Patten, T. E. *Langmuir* **2001**, *17*, 4479–4481.

- (21) Jeyaprakash, J.; Samuel, S.; Dhamodharan, R.; Ruhe, J. *Macromol. Rapid Commun.* **2002**, *23*, 277–281.
- (22) Ohno, K.; Morinaga, T.; Koh, K.; Tsujii, Y.; Fukuda, T. *Macromolecules* **2005**, *38*, 2137–2142.
- (23) Baum, M.; Brittain, W. J. *Macromolecules* **2002**, *35*, 610–615.
- (24) Li, C.; Benicewicz, B. C. *Macromolecules* **2005**, *38*, 5929–5936.
- (25) Li, C.; Han, J.; Ryu, C. Y.; Benicewicz, B. C. *Macromolecules* **2006**, *39*, 3175–3183.
- (26) Akcora, P.; Liu, H.; Kumar, S. K.; Moll, J.; Li, Y.; Benicewicz, B. C.; Schadler, L. S.; Acehan, D.; Panagiotopoulos, A. Z.; Pryamitsyn, V.; Ganesan, V.; Ilavsky, J.; Thiagarajan, P.; Colby, R. H.; Douglas, J. F. *Nat. Mater.* **2009**, *8*, 354–359.